

# UCSF

## UC San Francisco Previously Published Works

### Title

A culture system to study oligodendrocyte myelination processes using engineered nanofibers.

### Permalink

<https://escholarship.org/uc/item/1f4145x8>

### Journal

Nature Methods, 9(9)

### Authors

Lee, Seonok  
Leach, Michelle  
Redmond, Stephanie  
[et al.](#)

### Publication Date

2012-09-01

### DOI

10.1038/nmeth.2105

Peer reviewed



Published in final edited form as:

*Nat Methods*. 2012 September ; 9(9): 917–922. doi:10.1038/nmeth.2105.

## A culture system to study oligodendrocyte myelination-processes using engineered nanofibers

Seonok Lee<sup>1</sup>, Michelle K. Leach<sup>2</sup>, Stephanie A. Redmond<sup>1</sup>, S.Y. Christin Chong<sup>1</sup>, Synthia H. Mellon<sup>3</sup>, Samuel J. Tuck<sup>4</sup>, Zhang-Qi Feng<sup>2</sup>, Joseph M. Corey<sup>2,4,5,\*</sup>, and Jonah R. Chan<sup>1,\*</sup>

<sup>1</sup>Department of Neurology and Program in Neuroscience, University of California San Francisco, San Francisco, CA 94158

<sup>2</sup>Department of Biomedical Engineering, University of Michigan, Ann Arbor, MI 48109

<sup>3</sup>Departments of Obstetrics, Gynecology and Reproductive Sciences, University of California, San Francisco, San Francisco, CA 94143

<sup>4</sup>Department of Neurology, University of Michigan, Ann Arbor, MI 48109

<sup>5</sup>Geriatric Research, Education and Clinical Center, Veterans Affairs Ann Arbor Healthcare Center, Ann Arbor, MI 48105

### Abstract

Current methods for studying central nervous system myelination necessitate permissive axonal substrates conducive for myelin wrapping by oligodendrocytes. We have developed a neuron-free culture system in which electron-spun nanofibers of varying sizes substitute for axons as a substrate for oligodendrocyte myelination, thereby allowing manipulation of the biophysical elements of axonal-oligodendroglial interactions. To investigate axonal regulation of myelination, this system effectively uncouples the role of molecular (inductive) cues from that of biophysical properties of the axon. We use this method to uncover the causation and sufficiency of fiber diameter in the initiation of concentric wrapping by rat oligodendrocytes. We also show that oligodendrocyte precursor cells display sensitivity to the biophysical properties of fiber diameter and initiate membrane ensheathment prior to differentiation. The use of nanofiber scaffolds will enable screening for potential therapeutic agents that promote oligodendrocyte differentiation and myelination as well as provide valuable insight into the processes involved in remyelination.

---

Users may view, print, copy, download and text and data- mine the content in such documents, for the purposes of academic research, subject always to the full Conditions of use: [http://www.nature.com/authors/editorial\\_policies/license.html#terms](http://www.nature.com/authors/editorial_policies/license.html#terms)

\*To whom correspondence should be addressed; Dr. Jonah R. Chan, Department of Neurology and Program in Neuroscience, University of California San Francisco, 600 16<sup>th</sup> St. S576, Box 2280, San Francisco, CA 94143, Tel.: 415-514-9818, Fax: 415-514-4112, [jonah.chan@ucsf.edu](mailto:jonah.chan@ucsf.edu). Dr. Joseph Corey, [coreyj@med.umich.edu](mailto:coreyj@med.umich.edu).

#### Author Contributions

S.L., M.K.L., S.A.R., S.Y.C.C. and J.R.C performed experiments. S.L., M.K.L., S.H.M., S.J.T. Z.F. J.M.C. and J.R.C. provided reagents. S.L., M.K.L., S.A.R., S.Y.C.C., S.H.M., S.J.T. Z.F. J.M.C. and J.R.C. provided intellectual contributions. S.L. and J.R.C analyzed the data and wrote the paper.

#### Competing Financial Interests

The authors declare no competing financial interests.

## Keywords

fiber diameter; oligodendrocyte; myelination

---

## Introduction

One of the major hurdles when studying neuronal-glia interactions is trying to understand how two different cell types communicate effectively to accomplish a particular task. Myelination is the result of complex neuronal-glia interactions and is necessary for the efficient and rapid transmission of action potentials throughout the vertebrate nervous system. During development of the central nervous system (CNS), neurons and oligodendroglia interact with each other in numerous ways to achieve precise and timely myelination. It is generally accepted that inductive and/or inhibitory signals produced by axons control whether they will become myelinated<sup>1</sup>. Neurons also modulate proliferation and migration of oligodendrocyte precursor cells (OPCs) by providing mitogenic cues<sup>2</sup> and trophic factors<sup>3</sup>. Conversely, oligodendroglia support the function and the wellbeing of neurons<sup>4, 5</sup>. Due to the intimate nature of neuronal-oligodendroglial interactions, it is challenging to study certain processes related to myelination using in vitro co-culture methods, as these systems make it hard to uncouple indirect (neuronal) from direct (oligodendroglial) effects when axonal-oligodendroglial interactions are manipulated.

It is well established that large diameter axons tend to be myelinated while small diameter axons remain unmyelinated<sup>6</sup>. This correlative observation combined with the finding that increasing axon diameter stimulates myelination of normally unmyelinated axons<sup>7</sup> suggests that axonal fiber diameter may play an important role in regulating myelination. However, demonstrating causation or sufficiency in the contribution of axonal fiber diameter on myelination remains elusive, especially as the presence of molecular cues persist continuously along axons. Previous co-culture setups used to study myelination do not allow discriminating between diameter-dependent molecular signaling mechanisms and the biophysical property of fiber diameter itself. Therefore, uncoupling axon diameter from molecular cues expressed on the surface of axons is currently unachievable as the presence and degree of molecular signaling may be directly linked to axon caliber. In the peripheral nervous system (PNS), for example, production of neuregulin 1 type III (NRG) above a certain threshold by the axons dictates initiation of myelination by Schwann cells and NRG levels are thought to be dependent on axon diameter, providing a mechanism by which axon diameter controls the initiation of myelination. On the other hand, CNS oligodendrocytes, do not seem to respond to NRG1 levels to initiate axonal wrapping and the role of axon caliber on triggering myelination in the CNS remains unclear. Evaluating the causal relationship between axon diameter and oligodendrocyte myelination is complicated further, by the fact that axon diameters can change in an organism over time. Myelination promotes radial growth of axons during development<sup>8-10</sup>, and the longitudinal expansion of myelin internodes associated with the age-related growth of vertebrates decreases the overall diameter of the axon<sup>11</sup>. Effectively uncoupling the role of fiber diameter from an axonal signal necessitates manipulation of one without the other.

Recent efforts to investigate the need for axonal signals for the initiation of oligodendrocyte myelination reveal that initiation of myelination does not depend on axonal signals and may in fact be due to a permissive axonal environment, as oligodendrocytes myelinate paraformaldehyde-fixed axons<sup>12</sup>. To further investigate this phenomenon and to overcome previously mentioned obstacles we have developed an alternative culture system to study myelination-processes and use it to examine the biophysical role of fiber diameter on the initiation of myelination in the absence of molecular cues. To this end, we have utilized electron-spinning technology to generate polystyrene nanofibers as an artificial scaffold for oligodendrocyte myelination<sup>13, 14</sup>. Previous studies utilizing either glass microfibers<sup>15</sup> and/or Vicryl nanofibers<sup>16</sup> obtained promising results with oligodendrocytes ensheathing and wrapping the fibers, however, the influence of fiber diameter was not examined. By engineering nanofibers with varying diameters (0.2 to 4.0  $\mu\text{m}$ ), we demonstrate that fiber diameter is sufficient for initiating concentric wrapping by rat primary oligodendrocyte cultures. Fibers were examined by light and electron microscopy and the minimum fiber diameter threshold was quantified and determined to be 0.4  $\mu\text{m}$ . Oligodendrocytes show a preference for wrapping and ensheathing fibers of diameters larger than 0.5  $\mu\text{m}$ , with a 5-fold increase in the frequency of myelin-like segments formed by oligodendrocytes in these fibers. Further studies show that both OPCs and mature oligodendrocytes exhibit similar sensitivities to the biophysical properties of fiber diameter and that OPCs have the capacity to ensheath fibers prior to the expression of differentiation markers such as myelin basic protein (MBP).

The use of nanofibers in this reduced culture system allows unique studies related to myelination and has revealed the causal nature and sufficiency of fiber diameter on oligodendrocyte wrapping. This culture setup provides new opportunities to uncouple the axonal and glial contribution on myelination and should impart valuable insight into the identification of potential therapeutic strategies for remyelination.

## Results

### Myelination does not require dynamic axonal signaling

In order to examine myelination by oligodendrocytes *in vitro*, in the past we have utilized a co-culture system with dorsal root ganglion (DRG) neurons and purified rat primary OPCs<sup>12, 17, 18</sup>. Axons formed by DRGs are normally small in diameter and exist as either unmyelinated or thinly myelinated sensory fibers *in vivo*<sup>19</sup>. However, DRG axons hypertrophy when cultured in saturating concentrations of the neurotrophin nerve growth factor, resulting in an increase in their axon diameter (1–2  $\mu\text{m}$ ) (data not shown). This range of axon diameter is similar to myelinated axons in the CNS<sup>20</sup> and allows for the establishment of a robust co-culture model to study oligodendrocyte myelination *in vitro*<sup>21</sup>. Upon seeding onto DRGs, OPCs associate tightly with axons on which they proliferate rapidly until reaching a critical density (Supplementary Fig. 1a–d). Afterwards, the OPCs undergo a population-wide differentiation and myelinate axons<sup>12</sup> (Supplementary Fig. 1e,f), similar to physiological processes during oligodendroglial development. We previously reported that OPCs cultured on paraformaldehyde-fixed DRGs maintain the capacity to differentiate and myelinate axons similarly to live axons<sup>12</sup> (Supplementary Fig. 1g–i). This

finding demonstrates that initiation of myelination does not require dynamic axonal signaling and it suggests the presence of a permissive axonal environment for myelination. But this co-culture setup does not allow controlled manipulations of the biophysical properties regulating axon-oligodendroglial interactions. And in particular, it could not be used to address the question of whether the fiber diameter of axons represents the permissive aspect of the axonal environment that initiates myelination.

### Electron-spun polystyrene nanofibers for myelination studies

In order to develop an alternative culture model to overcome the limitations of previous culture systems and address this question, we engineered poly-L-lactic acid (PLLA) aligned electron-spun polystyrene nanofibers with diameters ranging from 0.2  $\mu\text{m}$  to 4.0  $\mu\text{m}$ <sup>13, 14</sup> (Fig. 1a, b). It has previously been observed that most of the myelinated axons in the mammalian CNS range in diameter from 0.3  $\mu\text{m}$  to 2  $\mu\text{m}$ , and that oligodendrocytes have the capacity to myelinate axons as large as 15  $\mu\text{m}$  in diameter<sup>20, 22</sup>. Therefore, the diameter range of our nanofibers represents a physiologically relevant mixture of axon calibers detected *in vivo*. We observed that OPCs cultured on poly-lysine-coated nanofibers showed similar behaviors as those observed in previous co-culture models using fixed or live DRGs<sup>12</sup> (Supplementary Figure 1). OPCs were cultured in the presence of platelet-derived growth factor (PDGF), a potent mitogen for OPCs, and were seen to closely align with the fibers and proliferate. OPCs rapidly occupy all of the fiber area before undergoing differentiation into MBP expressing mature oligodendrocytes (Fig. 1c–f). To quantify the proliferation and differentiation of OPCs on nanofibers, we analyzed the number of PDGFR $\alpha$  positive OPCs and MBP positive oligodendrocytes over a two-week period in culture (Fig. 1g,h). The results show that OPCs cultured on nanofibers proliferate until reaching a critical density prior to differentiation, mirroring the temporal and spatial progression of OPCs cultured on axons. To examine the functional role of axonal fiber diameter, OPCs were cultured on small (0.2–0.4  $\mu\text{m}$ ) and large diameter (2.0–4.0  $\mu\text{m}$ ) fibers (Fig. 2a,b). While OPCs efficiently differentiate on the small fibers, they only extend their processes and form membrane sheets but do not initiate wrapping (Fig. 2a, Supplementary Fig. 2d–g). In contrast, oligodendroglia cultured on larger diameter fibers differentiate, concentrically wrap the fibers (Fig. 2b) and form myelin-like segments of multiple compact membrane wraps as visualized by electron microscopy (Fig. 2c–e). It is important to note that while compact myelin is observed, it is infrequently detected. In fact, the majority of the myelin-like segments surrounding the fibers are aberrantly organized, with few wraps of membrane and cytoplasm remaining between the wraps. Additionally, a correlation between the number of wraps and the caliber of the fiber was not observed, indicating the importance of the axonal signals for myelin compaction and for the establishment of the appropriate number of wraps of membrane in the multilamellar organization of the myelin sheath (Fig. 2c–e). However, we demonstrate that myelin proteins such as Myelin-Associated Glycoprotein (MAG) and Myelin Oligodendrocyte Glycoprotein (MOG) are present within the MBP-positive segments (Fig. 2f,g). While the localization of MAG can be detected along the length of the segment, it is enriched at segment margins (Fig 2f, arrow), suggestive of non-compact myelin-like structures. MOG expression is indicative of oligodendrocyte maturation and suggests that the myelin-like segments observed may indeed represent mature oligodendrocyte wrapping and not a premyelinating phenomenon. This data

demonstrates that fiber diameter is sufficient to initiate membrane wrapping by oligodendrocytes. To determine if this minimum threshold observation could be overcome by coating the fibers with different substrates, we coated small diameter fibers with laminin<sup>23</sup>, nectin-like protein 1 (Nectin1)<sup>24</sup>, poly-lysine and purified axonal membranes. None of the substrates, including axonal membranes, promoted wrapping of small diameter fibers by oligodendrocytes. The cells extended membrane sheets that spread between and/or on top of the fibers but did not wrap them (Supplementary Fig. 2d–g).

### Quantification of fiber diameter threshold and preference

Previous observations have demonstrated that fiber diameter is tightly correlated with the initiation of myelination *in vivo* and that the diameter of axons usually range from 1  $\mu\text{m}$  in the PNS and approximately 0.2–0.7  $\mu\text{m}$  in the CNS prior to myelination<sup>11, 20</sup>. To determine the minimum fiber diameter at which oligodendrocytes commence wrapping in our system, we analyzed oligodendrocytes cultured on nanofibers ranging from 0.2–4.0  $\mu\text{m}$  in diameter and quantified the total number of MBP-positive segments (Fig. 3a) normalized to the fiber distribution on each coverslip (Fig. 3b). We find that the minimum fiber diameter threshold for oligodendrocyte myelination is approximately 0.4  $\mu\text{m}$ , consistent with the observed axon caliber reported during development *in vivo*<sup>22</sup>. To demonstrate that diameter dependent wrapping of fibers is specific to oligodendrocytes, astrocytes were co-cultured on nanofibers (Supplementary Fig. 3a–c). We find that astrocytes extend long fiber-like membrane processes across and/or along the fibers but none of the membrane growth patterns resemble that of oligodendrocyte wrapping.

We then used this culture setup to investigate the relationship between initiation of wrapping and differentiation of OPCs. Typically, expression of MBP is a hallmark of oligodendrocyte differentiation and the formation of myelin segments on axons. It has been well accepted that MBP-positive mature oligodendrocytes wrap axons and form myelin but at what stage the oligodendroglial cells initiate ensheathment and wrapping remains unclear. We hypothesized that OPCs may demonstrate sensitivity for the minimum fiber diameter threshold and initially select and wrap fibers prior to MBP expression. Consistent with this hypothesis, we find that PDGFR $\alpha$ + / MBP–, indicative of OPCs that are still immature, extend membrane processes and ensheath only the larger diameter fibers (> 0.4  $\mu\text{m}$ ) (Fig. 3c,d,e). This ensheathment in the absence of MBP expression is confirmed by electron microscopy of the cultures (Fig. 3f). PDGFR $\alpha$ + segments are indeed OPCs that lack MBP expression (Supplementary Fig. 4a–c), albeit possessing morphologies that closely resemble that of MBP+ oligodendrocytes (Fig. 3c). Additionally, we purified galactosylceramide (GalC) positive mature oligodendrocytes from the postnatal rat brain and assessed their ability to wrap fibers with varying diameters (Supplementary Fig. 4d,e). Similar to OPCs, mature oligodendrocytes consistently wrap fibers with diameters above 0.4  $\mu\text{m}$  and cannot wrap fibers below this diameter threshold (Supplementary Fig. 4d,e).

As the minimum diameter threshold may represent the transition between permissive and non-permissive axonal environments, we set out to determine whether oligodendroglia display a preference for specific diameter fibers. This may provide some insight into the temporal regulation of myelination during mammalian brain development as many regions

of the CNS contain an assortment of small and large diameter axons<sup>22</sup>. Developmental studies have shown that the largest diameter axons from the spinal cord are the first to be myelinated, suggesting a potential oligodendroglial preference for larger diameter axons<sup>25</sup>. To investigate this preference for larger diameter axons we examined the developing optic nerve by electron microscopy. Initiation of compact myelination can be detected at postnatal day 8 (Supplementary Fig. 5a,b). Upon quantification of the diameters of the axons undergoing early myelination, we find that only axons with a diameter greater than 0.3  $\mu\text{m}$  show signs of being engaged in the initial stages of myelination. To test oligodendroglial preference for axonal diameter in our culture setup, we used PLLA-fibers engineered to display gradual changes in diameter continuously along the same fiber (Fig. 3g). We observed that oligodendrocytes display a preference for ensheathing and wrapping sections corresponding to larger fiber diameters (Fig. 3h). To quantify this preference, we used mixtures of polystyrene fibers with diameters ranging from 0–0.8  $\mu\text{m}$  and quantified the number of MBP+ or PDGFR $\alpha$ + segments wrapping each of the different fiber groups. We demonstrate that fibers with a diameter ranging from 0.5–0.6  $\mu\text{m}$  and 0.7–0.8  $\mu\text{m}$  display a respective 5- and 7-fold increase in the frequency of MBP+ or PDGFR $\alpha$ + segments as compared to smaller diameter fibers ranging from 0.3–0.4  $\mu\text{m}$  (Fig. 3i). This finding is consistent even when the small diameter fibers (0.2–0.4  $\mu\text{m}$ ), are overrepresented in the mixed fibers, suggesting that OPCs and oligodendrocytes prefer larger diameter fibers even if the smaller fibers are above minimum threshold (Supplementary Fig. 6).

### Quantification of cells in the cultures that ensheath or wrap fibers

We quantified the percentage of OPCs and oligodendrocytes that ensheath or wrap the fibers in our cultures (Fig. 4a–c). Approximately, 60% of OPCs and oligodendrocytes ensheath or wrap large diameter fibers (2.0–4.0  $\mu\text{m}$ ), whereas only approximately 5% ensheath or wrap fibers between 0.2–0.4  $\mu\text{m}$  in diameter (Fig. 4a). It must be noted that the few fibers that are ensheathed or wrapped belonging to this group are approximately 0.4  $\mu\text{m}$  (data not shown). While oligodendroglial cells consistently exhibit multipolar morphologies in vivo and when cultured with DRG axons, the cells cultured on the nanofiber platform display both bipolar and multipolar morphologies (Fig. 4d,e). This observation suggests that axonal cues may contribute to the morphology, process extension and/or stabilization of oligodendroglial cells. Nevertheless, both bipolar and multipolar oligodendroglial cells exhibit similar sensitivities to fiber diameter and readily ensheath and wrap the fibers when their diameters are larger than 0.3  $\mu\text{m}$  (Fig. 4d). Together, these findings suggest that OPCs and oligodendrocytes share a conserved sensitivity for the biophysical properties of fiber diameter and implicate a novel chronology of events for the myelination process, whereby differentiation in the context of protein and lipid expression occurs after selection and ensheathment of fibers by OPCs (Supplementary Fig. 7).

## Discussion

We show that OPCs cultured with poly-L-lysine-coated nanofibers tightly associate with the fibers and undergo proliferation until reaching a critical density prior to differentiation, mirroring processes observed when OPCs are cultured with live or fixed axons. We also demonstrate that OPCs display sensitivity to the biophysical properties of fiber diameter and

will select and ensheath fibers prior to the expression of myelin proteins, maintaining this ensheathment during proliferation (data not shown). Based on these observations, we hypothesize that during CNS development, OPCs proliferate until reaching some critical density, while concurrently selecting and ensheathing axons based on their diameter, prior to differentiation and myelination (Supplementary Fig. 7). We propose that differentiation represents the expression of the proteins and lipids that are paramount for formation of multilamellar structures and compact membrane wrappings indicative of the myelin sheath, and suggest that an OPC that differentiates into an oligodendrocyte in a permissive axonal environment will ultimately form myelin.

As we show in this work, the use of engineered nanofibers provides unique opportunities to study myelination processes and represents a complementary approach from current methodologies that rely on the presence of co-cultured neurons. These nanofiber scaffolds allow for the study of oligodendroglia dynamics and will enable the screening of therapeutic agents in a minimally-permissive environment without confounding neuronal contributions. As shown here, OPCs and oligodendrocytes are sensitive to a minimum fiber diameter threshold in order to initiate myelination-related processes. This finding may provide leads for the development of new strategies that promote remyelination after injury or/disease by ensuring the presence of a permissive axonal environment.

## Online Methods

### Electron-spinning nanofibers for myelination

Polymer nanofibers of varying diameter were generated by the electron-spinning method as described previously<sup>14, 26</sup>. Briefly, poly-L-lactic acid (PLLA) fibers were spun from a solution of 4% w/v PLLA dissolved in chloroform:dimethylformamide (9:1 v/v). The fluorescent dye sulforhodamine was added to the solution just prior to spinning at a concentration of 0.0025% w/v. The solution was pumped through a 6 cm long 25 gauge blunt metal tip placed 30 cm distant from the rapidly rotating collector wheel (25 cm diameter, 600 RPM). The metal tip was maintained at a voltage of +25 kV and the collector wheel was maintained at -2 kV. Polystyrene fibers were similarly spun from a solution of 30% w/v polystyrene in dichloromethane:dimethylformamide (1:1 v/v). A 1.5 cm blunt metal tip was maintained at +15 kV during spinning and the collector wheel remained at -2 kV. The diameter of the resulting polystyrene fibers was controlled by varying the speed of the collector (500–2000 RPM) as well as the distance between the tip and the collector (15–30 cm). During collection, electron-spun nanofibers were aligned and loosely attached electrostatically to 12mm glass coverslips and aligned at the surface of the collector. After spinning, silicone adhesive sealant (Dow Corning) was used to secure fibers to the coverslips. The fiber diameter was assessed by scanning electron microscopy (SEM) (Supplementary Fig. 1a–c). Fibers were sterilized by rinsing with 70% EtOH, washed with water, and then coated with the appropriate substrates prior to the seeding of oligodendroglia.



### Substrate coating of electron-spun nanofibers

Nanofibers were coated with poly-L-lysine (100 µg/ml) for 1 h, washed twice with water and air-dried. In some cases, this was followed by incubation with laminin (5 µg/ml) in DMEM at 37 °C for 2 h. Laminin was removed via one wash with DMEM before the seeding of OPCs. For Supplementary Fig. 1, DRG axonal membranes were purified using an adapted protocol<sup>27</sup>. Briefly, DRG cell bodies were excised, and the remaining axons were extracted in DPBS, subjected to freeze-thaw cycles before ultracentrifugation at 540,000 g for 1 h at 4 °C. The membrane pellet was resuspended in chemically-defined medium, sonicated, and incubated with the nanofibers overnight at 4 °C for proper adsorption. Unattached membranes were gently removed prior to the seeding of OPCs. For coating the fibers with Nectin1 protein, Nectin1-Fc fusion proteins (gift from Dr. E. Peles) were incubated overnight and washed extensively in DMEM (Invitrogen) prior to seeding OPCs.

### Isolation of primary rat oligodendrocytes

Immunopanning of OPCs and oligodendrocytes was performed as previously described<sup>17</sup>. Briefly, OPCs were purified from P7-P8 Sprague-Dawley rat brain cortices, whereas mature oligodendrocytes were purified from P9 rat brain cortices. Male and female sprague dawley rats pups and timed-pregnant female rats were ordered from Lawrence River 1–7 days before OPC isolation, and were housed in University of California, San Francisco (UCSF) specific pathogen free vivarium. Animals were housed and euthanized in accordance with all Institutional Animal Care and Use Committee (IACUC) and Laboratory Animal Resource Center (LARC) requirements as specified by the US National Institutes of Health. For immunopanning, Petri dishes were incubated overnight with goat anti-mouse IgG/M secondary antibodies (Jackson Laboratories) in 50 mM Tris-HCL, pH 9.5. Dishes were then rinsed and incubated at room temperature with primary antibodies against astrocyte cell surface protein, rat neural antigen-2 (Ran-2), galactosylceramide (GalC), and A2B5 (a marker for glial precursor cells) for the isolation of rat OPCs. Rat brain hemispheres were diced and dissociated with papain (Worthington, cat # 3119) at 37 °C. After trituration, cells were resuspended in a panning buffer (0.2% BSA in DPBS) and incubated at room temperature sequentially on three immunopanning dishes: for OPCs, Ran-2 and GalC were used for negative selection prior to positive selection with A2B5. For the purification of mature oligodendrocytes, Ran-2 and A2B5 were used for negative selection prior to positive selection with GalC. OPCs or oligodendrocytes were released from the final panning dish using 0.25% Trypsin (Invitrogen).

### Oligodendroglial-nanofiber cultures

250,000 rat primary oligodendroglial cells isolated from postnatal brains as described above, were cultured on substrate-coated nanofibers in chemically-defined medium composed of DMEM (Invitrogen) supplemented with B27 (Invitrogen), N2 (Invitrogen), penicillin-streptomycin (Invitrogen), N-acetyl-cysteine (Sigma-Aldrich), forskolin (Sigma-Aldrich) and 12.5 ng/ml PDGF-AA (Peprotech). Cultures were maintained for 15 days prior to analysis.

### Quantification of PDGFR $\alpha$ + or MBP+ segments on fibers

The distribution of nanofiber diameters (0.2–4.0  $\mu\text{m}$ ) on each coverslip was determined by scanning electron microscopy. Nanofibers on coverslips were subdivided into 4 categories based on the distribution of the fiber diameters: 1) 0.2–0.4  $\mu\text{m}$ , 2) 0.3–0.8  $\mu\text{m}$ , 3) 0.8–2  $\mu\text{m}$  and 4) 0.6–4.0  $\mu\text{m}$ . Fibers with diameters ranging from 0.2–4.0  $\mu\text{m}$  were used to determine threshold diameter for ensheathment and wrapping, and fibers ranging from 0.2–0.8  $\mu\text{m}$  were used to quantify preference. OPC ensheathment was analyzed by quantifying the number of PDGFR $\alpha$ + segments while oligodendrocyte wrapping was analyzed by quantifying the number of MBP+ segments covering the fibers. All segments were defined by the complete ensheathment of a fiber for a length greater than 30  $\mu\text{m}$ . For all quantifications, the number of PDGFR $\alpha$  and MBP segments represents the mean of at least three independent experiments. Three coverslips were quantified per category of fibers (1–4) and 20–30 fields per coverslip were acquired ( $n = 3$ ). Finally, the total number of segments was normalized to the distribution of the fiber diameters from each category (1–4). Statistical significance across all categories was evaluated with Tukey post hoc comparison after one-way ANOVA ( $P < 0.001$ ).

### OPC-DRGs co-cultures

OPC-DRG co-cultures were prepared as previously described<sup>17</sup>. Briefly, DRG neurons from E15 Sprague-Dawley rats were dissociated, plated (150,000 cells per 25 mm cover glass), and purified on collagen-coated coverslips in the presence of 100 ng/ml NGF (AbD Serotec). Neurons were maintained for three weeks and washed with DMEM (Invitrogen) extensively to remove any residual NGF before seeding OPCs. Co-cultures were grown in chemically-defined medium composed of DMEM (Invitrogen) supplemented with B27 (Invitrogen), N2 (Invitrogen), penicillin-streptomycin (Invitrogen), N-acetyl-cysteine (Sigma-Aldrich), and forskolin (Sigma-Aldrich). Culturing OPCs on fixed axons has been described previously<sup>12</sup>. Briefly, DRG neuronal cultures were washed gently with DPBS (Invitrogen) and fixed with 4% paraformaldehyde (PFA) (Electron Microscopy Sciences) solution for 15 min. After the removal of PFA, neurons were washed extensively with DPBS and then L15 (Invitrogen) + 10% fetal bovine serum (FBS) (Invitrogen) prior to seeding of OPCs.

### Immunostaining

Cultures were fixed with 4% PFA, dehydrated, permeabilized and blocked by incubation with 20% goat serum (Sigma-Aldrich) and 0.2% Triton X-100 (Sigma-Aldrich) in PBS. Differentiated oligodendrocytes and myelin were detected with a rat monoclonal anti-MBP antibody (Millipore), and OPCs were detected with a rabbit monoclonal anti-PDGFR $\alpha$  antibody (gift from Dr. William B. Stallcup). Astrocytes were detected with rabbit anti-GFAP antibody (Millipore) and axons were detected with a mouse anti-neurofilament (NF) antibody (Covance). The Alexa Fluor 488, 594 and 647 anti-rat, -rabbit, and -mouse IgG secondary antibodies (Invitrogen) were used for fluorescence detection. Cell nuclei were identified with DAPI (Vector Labs). 20X z-stack projections were acquired at 0.8  $\mu\text{m}$  intervals using the Zeiss Axio Imager Z1 with ApoTome attachment and Axiovision software.

### Preparation of nanofiber cultures for electron microscopy

For analysis of myelination on polystyrene fibers, cultures were fixed with 4% PFA for 20 min, then stained with 1% osmium tetroxide for 1 h at 4°C and counterstained with 1% uranyl acetate overnight. Samples were rinsed with distilled water and dehydrated in a series of ethanol dehydration treatments (50, 70, 95, and 100% EtOH). Embedding was performed in a 1:1 resin (EMBed-812, DDSA, NMA and BDMA; Electron Microscopy Sciences) and 2-hydroxypropylmethacrylate (HPMA; Electron Microscopy Sciences) mix for 1 h at room temperature, followed by a 2:1 resin/HPMA mix overnight at room temperature, and 100% resin for 3 h at room temperature. Samples were placed in fresh resin and cured overnight at 65°C. Ultrathin sections (70 nm) were obtained by Mei lie Wong at the W.M. Keck Foundation Advanced Microscopy Laboratory at the University of California, San Francisco, and visualized with a JEM1400 Electron Microscope (JEOL) in the Zilkha Neurogenetic Institute at the University of Southern California.

### Preparation of fixed OPC/DRGs co-cultures for electron microscopy

Preparing OPC/fixed-DRGs co-cultures for EMs has been described previously<sup>12</sup>. Briefly, high density OPCs co-cultured with fixed DRGs for seven days were fixed in 2% glutaraldehyde, stained with 1% osmium tetroxide, and counterstained with 1% uranyl acetate overnight. Cocultures were subsequently rinsed with distilled water and dehydrated in a series of ethanol solutions (50, 70, 95 and 100% EtOH). Samples were then embedded in resin (EMBed-812, Electron Microscopy Sciences). Ultrathin sections (70 nm) were obtained from the Norris Center Cell and Tissue Imaging Core at the University of Southern California, Keck School of Medicine, and visualized with a JEM1400 Electron Microscope (JEOL) in the Zilkha Neurogenetic Institute.

### Preparation of optic nerves for electron microscopy

Postnatal mice were deeply anesthetized with a mixture of ketamine and xylazine and transcardially perfused with 4% paraformaldehyde in PBS. As previously described<sup>28</sup>, optic nerves were dissected and postfixed in the same perfusion solution at 4°C overnight. All nerves were stained with 1% osmium tetroxide for 1 h at 4°C, counterstained with 1% uranyl acetate overnight, then dehydrated through ascending ethanol solutions (50, 70, 95 and 100% ETOH). Samples were then embedded in a 1:1 resin (EMBed-812; Electron Microscopy Sciences) and propylene oxide (Electron Microscopy Sciences) mix for 1 h at room temperature, followed by a 2:1 resin/propylene oxide mix overnight at room temperature. Nerves were then placed in 100% resin for 3 h at room temperature. Ultrathin sections (70 nm) were obtained from the Norris Center Cell and Tissue Imaging Core at the University of Southern California, Keck School of Medicine, and visualized with a JEM1400 Electron Microscope (JEOL) in the Zilkha Neurogenetic Institute. For quantification, over 300 axons from two different optic nerve bundles were analyzed and the percentage of unmyelinated and myelinated axons were obtained. Error bars represent SD. Scale bar, 0.5 μm

## Supplementary Material

Refer to Web version on PubMed Central for supplementary material.

## Acknowledgments

We thank Dr. William Stallcup for the rabbit anti-PDGFR $\alpha$  antibody, Drs. Ralf Langen and Mario Isas for assistance, advice and support with the electron microscopy, the Chan lab members and the MS Research Group at UCSF for encouragement, advice and insightful discussions. This work was supported by the US National Multiple Sclerosis Society Career Transition Award (TA 3008A2/T), the Harry Weaver Neuroscience Scholar Award (JF 2142-A2/T), and the NIH/NINDS (NS062796-02) to J.R.C.

## References

1. Colello RJ, Pott U. Signals that initiate myelination in the developing mammalian nervous system. *Mol Neurobiol.* 1997; 15:83–100. [PubMed: 9396006]
2. Fruttiger M, Calver AR, Richardson WD. Platelet-derived growth factor is constitutively secreted from neuronal cell bodies but not from axons. *Curr Biol.* 2000; 10:1283–1286. [PubMed: 11069109]
3. Jiang F, Frederick TJ, Wood TL. IGF-I synergizes with FGF-2 to stimulate oligodendrocyte progenitor entry into the cell cycle. *Dev Biol.* 2001; 232:414–423. [PubMed: 11401402]
4. Nave KA, Trapp BD. Axon-glia signaling and the glial support of axon function. *Annu Rev Neurosci.* 2008; 31:535–561. [PubMed: 18558866]
5. Nave KA. Myelination and support of axonal integrity by glia. *Nature.* 2010; 468:244–252. [PubMed: 21068833]
6. Friede RL. Control of myelin formation by axon caliber (with a model of the control mechanism). *J Comp Neurol.* 1972; 144:233–252. [PubMed: 5029134]
7. Voyvodic JT. Target size regulates calibre and myelination of sympathetic axons. *Nature.* 1989; 342:430–433. [PubMed: 2586612]
8. de Waegh SM, Lee VM, Brady ST. Local modulation of neurofilament phosphorylation, axonal caliber, and slow axonal transport by myelinating Schwann cells. *Cell.* 1992; 68:451–463. [PubMed: 1371237]
9. Garcia ML, et al. NF-M is an essential target for the myelin-directed “outside-in” signaling cascade that mediates radial axonal growth. *J Cell Biol.* 2003; 163:1011–1020. [PubMed: 14662745]
10. Garcia ML, et al. Phosphorylation of highly conserved neurofilament medium KSP repeats is not required for myelin-dependent radial axonal growth. *J Neurosci.* 2009; 29:1277–1284. [PubMed: 19193875]
11. Waxman SG, Bennett MV. Relative conduction velocities of small myelinated and non-myelinated fibres in the central nervous system. *Nat New Biol.* 1972; 238:217–219. [PubMed: 4506206]
12. Rosenberg SS, Kelland EE, Tokar E, De la Torre AR, Chan JR. The geometric and spatial constraints of the microenvironment induce oligodendrocyte differentiation. *Proc Natl Acad Sci U S A.* 2008; 105:14662–14667. [PubMed: 18787118]
13. Gertz CC, et al. Accelerated neuritogenesis and maturation of primary spinal motor neurons in response to nanofibers. *Dev Neurobiol.* 2010; 70:589–603. [PubMed: 20213755]
14. Leach MK, Feng ZQ, Tuck SJ, Corey JM. Electrospinning fundamentals: optimizing solution and apparatus parameters. *J Vis Exp.* 2011
15. Bullock PN, Rome LH. Glass micro-fibers: a model system for study of early events in myelination. *J Neurosci Res.* 1990; 27:383–393. [PubMed: 2097381]
16. Howe CL. Coated glass and vicryl microfibers as artificial axons. *Cells Tissues Organs.* 2006; 183:180–194. [PubMed: 17159344]
17. Chan JR, et al. NGF controls axonal receptivity to myelination by Schwann cells or oligodendrocytes. *Neuron.* 2004; 43:183–191. [PubMed: 15260955]
18. Chong SY, et al. Neurite outgrowth inhibitor Nogo-A establishes spatial segregation and extent of oligodendrocyte myelination. *Proc Natl Acad Sci U S A.* 2011
19. Ruit KG, Elliott JL, Osborne PA, Yan Q, Snider WD. Selective dependence of mammalian dorsal root ganglion neurons on nerve growth factor during embryonic development. *Neuron.* 1992; 8:573–587. [PubMed: 1550679]

20. Remahl S, Hildebrand C. Changing relation between onset of myelination and axon diameter range in developing feline white matter. *J Neurol Sci.* 1982; 54:33–45. [PubMed: 7077354]
21. Kleitman, N.; Wood, PM.; Bunge, RP. *Culturing Nerve Cells.* BG; GK, editors. MIT; Cambridge, MA: 1991. p. 337-377.
22. Fanarraga ML, Griffiths IR, Zhao M, Duncan ID. Oligodendrocytes are not inherently programmed to myelinate a specific size of axon. *J Comp Neurol.* 1998; 399:94–100. [PubMed: 9725703]
23. Colognato H, Ramachandrapa S, Olsen IM, ffrench-Constant C. Integrins direct Src family kinases to regulate distinct phases of oligodendrocyte development. *J Cell Biol.* 2004; 167:365–375. [PubMed: 15504915]
24. Spiegel I, Peles E. A novel method for isolating Schwann cells using the extracellular domain of Nectin1. *J Neurosci Res.* 2009; 87:3288–3296. [PubMed: 19125407]
25. Schwab ME, Schnell L. Region-specific appearance of myelin constituents in the developing rat spinal cord. *J Neurocytol.* 1989; 18:161–169. [PubMed: 2471819]
26. Corey JM, et al. The design of electrospun PLLA nanofiber scaffolds compatible with serum-free growth of primary motor and sensory neurons. *Acta Biomater.* 2008; 4:863–875. [PubMed: 18396117]
27. Grimes ML, et al. Endocytosis of activated TrkA: evidence that nerve growth factor induces formation of signaling endosomes. *J Neurosci.* 1996; 16:7950–7964. [PubMed: 8987823]
28. Lewallen KA, et al. Assessing the role of the cadherin/catenin complex at the Schwann cell-axon interface and in the initiation of myelination. *J Neurosci.* 2011; 31:3032–3043. [PubMed: 21414924]

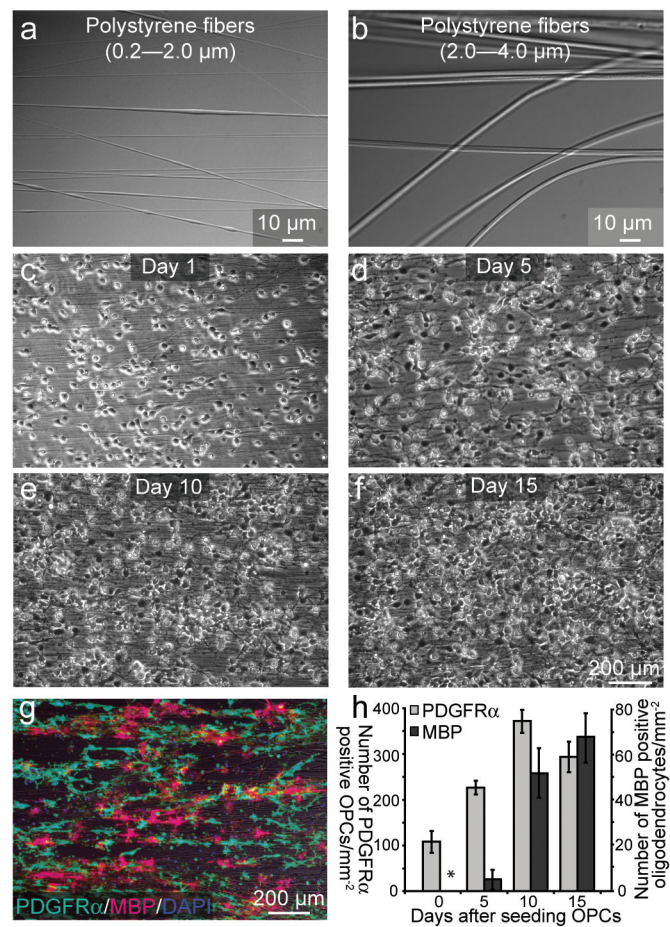


**Figure 1.**

Temporal and spatial behavior of OPCs on polystyrene fibers are similar to that of OPCs on live axons. (a–f) Phase contrast images of (a, b) polystyrene nanofibers that range in diameter from (a) 0.2–2.0 μm (b) 2.0–4.0 μm. (c–f) Bright-field images of cultured OPCs in the presence of exogenous PDGF and polystyrene fibers (0.2–0.4 μm) over 15 days in vitro (DIV). (g) Immunostaining of 10 DIV cultures against the OPC marker PDGFR $\alpha$  and MBP, which labels mature oligodendrocytes. (h) Quantification of the number of PDGFR $\alpha$ + OPCs and MBP+ oligodendrocytes per millimeter squared on nanofibers as a function of time ( $n = 3$ , mean + SD). Error bars represent SD. Scale bars, 10 μm (a, b), 200 μm (c–g).

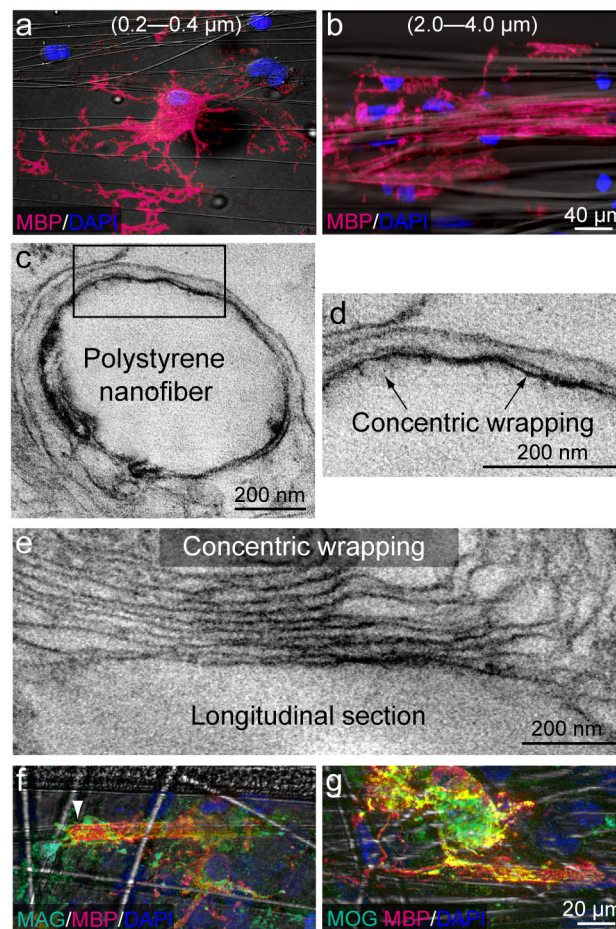


**Figure 2.**

Fiber diameter is sufficient to initiate myelination. **(a,b)** Immunostaining of cultures for MBP and DAPI in the presence of small **(a)**, 0.2–0.4 μm and large **(b)**, 2.0–4.0 μm diameter fibers. **(c–e)** Electron micrographs of an oligodendrocyte wrapping a large diameter nanofiber. **(d)** Higher magnification of the inset box found in **(c)**. Arrows indicate concentric wrapping of membrane. **(e)** A high magnification image of a longitudinal section illustrating an oligodendrocyte wrapping multiple layers of membrane around a large diameter nanofiber. **(f, g)** Immunostaining of oligodendrocytes cultured on large diameter nanofibers against the myelin proteins Myelin-Associated Glycoprotein (MAG) and Myelin Oligodendrocyte Glycoprotein (MOG). Scale bars, 40 μm **(a, b)**, 200 nm **(c–e)**, 20 μm **(f, g)**.

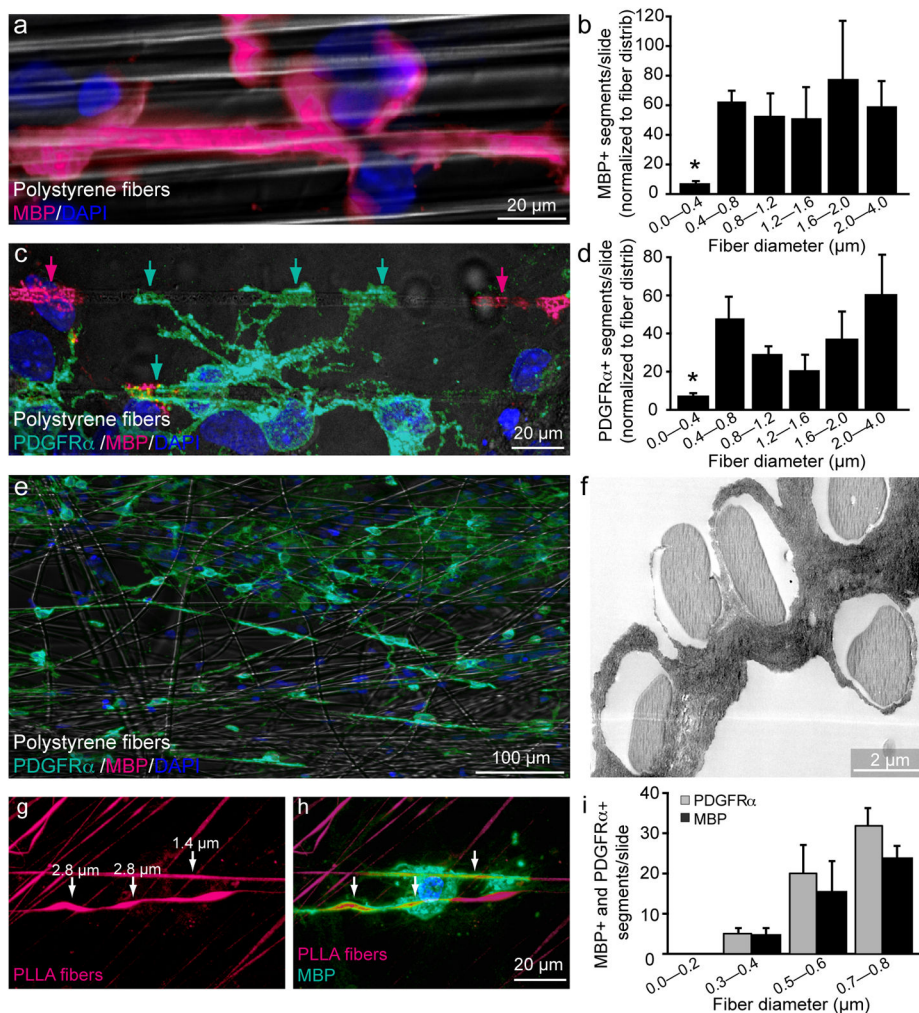


**Figure 3.**

Quantification of fiber diameter threshold and size preference for ensheathment and wrapping. **(a)** Immunostaining showing a magnified view of an MBP+ segment formed around a large diameter fiber (2.0–4.0 μm). Cell nuclei are labeled with DAPI **(b)** Quantification of the number of MBP+ segments normalized to the distribution of fiber diameters ( $n = 3$ , mean  $\pm$  SEM.). (\* represents  $P < 0.001$ , Tukey post hoc comparison after one-way ANOVA). **(c)** Immunostaining for PDGFR $\alpha$  and MBP illustrates an PDGFR $\alpha$ +/MBP- OPC in green ensheathing multiple large diameter fibers, as indicated by arrows. PDGFR $\alpha$ -/MBP+ oligodendrocyte segments in magenta (indicated by magenta arrows) are adjacent to the PDGFR $\alpha$ +/MBP- ensheathment. **(d)** Quantification of PDGFR $\alpha$ + segments normalized to fiber diameter distribution ( $n = 3$ , mean  $\pm$  SEM)(\* represents  $P < 0.001$ , Tukey post hoc comparison after one-way ANOVA) **(e)** Low magnification image of OPC-fiber cultures immunostained at 5 DIV for PDGFR $\alpha$ , MBP and DAPI. **(f)** Electron micrograph of OPC-fiber cultures illustrating ensheathment of multiple large diameter fibers. **(g)** Image of fibers engineered to display a range of diameter sizes continuously along the same fiber and conjugated with rhodamine. **(h)** Immunostaining for MBP illustrates an oligodendrocyte wrapping regions of the fiber that are larger in diameter as indicated by



arrows. **(i)** Quantification of fiber diameter preference by binning the number of MBP+ and PDGFR $\alpha$ + segments in 0.2  $\mu$ m intervals from 0 to 0.8  $\mu$ m ( $n=3$ , mean  $\pm$  SEM). ( $P < 0.001$ , Tukey post hoc comparison after one-way ANOVA). Scale bars, 20  $\mu$ m (**a, c, h**), 100  $\mu$ m (**e**), 2  $\mu$ m (**f**).

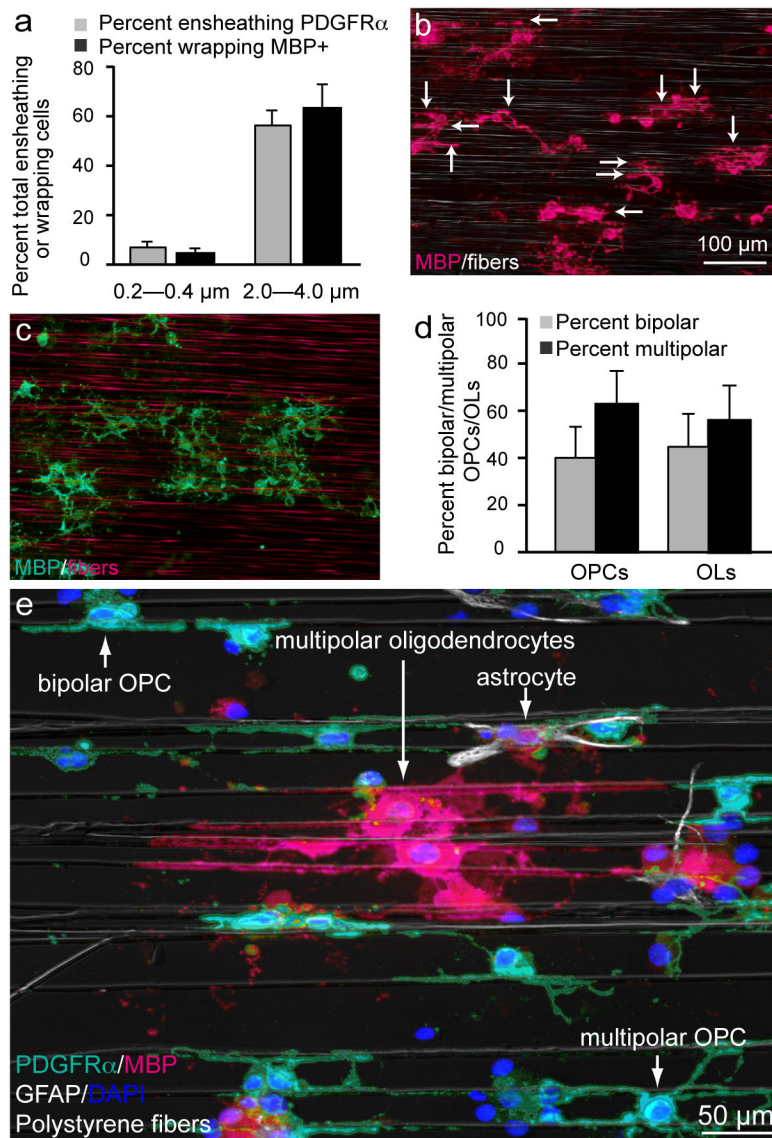


**Figure 4.**

The majority of the cells in the cultures are capable of ensheathing and wrapping fibers above a minimum threshold. **(a)** Quantification of the percent of OPCs that ensheat or wrap small or large diameter fibers ( $n = 5$ , mean  $\pm$  SD). Scale bar, 50  $\mu$ m **(b, c)** Low magnification images of purified oligodendroglial-fiber cultures immunostained at 10 DIV for MBP. **(b)** Image of cultures in the presence of large (2.0–4.0  $\mu$ m) diameter fibers. Fibers can be seen by phase contrast. Arrows indicate individual myelin-like segments. **(c)** Image of cultures in the presence of small diameter fibers (0.2–0.4  $\mu$ m). As it is difficult to visualize small diameter fibers by phase contrast microscopy, they are labeled with rhodamine to allow for clear visualization. **(d)** Quantification of the differing morphologies of the oligodendroglial cells cultured on the nanofibers ( $n = 4$ , mean  $\pm$  SD). Scale bars, 100  $\mu$ m. **(e)** Low magnification image of purified oligodendroglial-fiber cultures immunostained at 10 DIV stained for glial fibrillary acidic protein (GFAP;white), a marker for

contaminating astrocytes, PDGFR $\alpha$  (turquoise), MBP (magenta), and DAPI (blue). Fibers can be seen by phase contrast. Arrows indicate each cell type and different morphologies.

Author Manuscript

Author Manuscript

Author Manuscript

Author Manuscript